

Exposing Fine-grained Adversarial Vulnerability of Face Anti-spoofing Models

Songlin Yang^{1,2}, Wei Wang^{2*}, Chenye Xu³, Bo Peng², and Jing Dong²

¹ School of Artificial Intelligence, University of Chinese Academy of Sciences, China

² Center for Research on Intelligent Perception and Computing, CASIA, China

³ SenseTime Group Limited, China

yangsonglin2021@ia.ac.cn, xuchenye@sensetime.com,

wwang, jdong, bo.peng@nlpr.ia.ac.cn

Abstract. Adversarial attacks seriously threaten the high accuracy of face anti-spoofing models. Little adversarial noise can perturb their classification of live and spoofing. The existing adversarial attacks fail to figure out which part of the target face anti-spoofing model is vulnerable, making adversarial analysis tricky. So we propose fine-grained attacks for exposing adversarial vulnerability of face anti-spoofing models. Firstly, we propose Semantic Feature Augmentation (SFA) module, which makes adversarial noise semantic-aware to live and spoofing features. SFA considers the contrastive classes of data and texture bias of models in the context of face anti-spoofing, increasing the attack success rate by nearly 40% on average. Secondly, we generate fine-grained adversarial examples based on SFA and the multitask network with auxiliary information. We evaluate three annotations (facial attributes, spoofing types and illumination) and two geometric maps (depth and reflection), on four backbone networks (VGG, Resnet, Densenet and Swin Transformer). We find that facial attributes annotation and state-of-art networks fail to guarantee that models are robust to adversarial attacks. Such adversarial attacks can be generalized to more auxiliary information and backbone networks, to help our community handle the trade-off between accuracy and adversarial robustness.

Keywords: Face anti-spoofing, adversarial attacks, biometrics

1 Introduction

Face anti-spoofing is significantly important to the credibility of face recognition systems, which aims to determine whether a presented face is live or spoofing. If the face anti-spoofing part is unreliable, malicious attackers can use photos and videos of your face to unlock your mobile phone or other biometric authentication systems. Furthermore, auxiliary information (annotations and geometric information) can greatly boost the performance and generalizability of face anti-spoofing across a wide range of spoofing attacks [46], as well as state-of-art model structures [43].

However, the emergence of adversarial examples poses a fatal threat to face anti-spoofing models. Adversarial attacks like Fast Gradient Sign Method (FGSM) [14] and Project Gradient Descent (PGD) [26], can easily mislead the target model, making the model output a wrong classification result with high confidence. For example, a image of your photo could have been classified as spoofing input, but this image will be classified as live input after modified by FGSM [14].

Adversarial learning [8] takes adversarial examples as training data for defense, but this will degrade the performance of face anti-spoofing models on clean data. Another solution is to select auxiliary information and backbones with better adversarial robustness. But evaluating adversarial robustness in the context of face anti-spoofing has rarely been studied. The core of both solutions lies in how to generate adversarial examples. So studying attacks (generating adversarial examples) is significantly necessary before launching defense. To tackle this important problem, we thoroughly study adversarial attacks from the following two questions:

What should we consider when generating adversarial examples to expose adversarial vulnerability in the context of face anti-spoofing?

The answer is to consider both data and models. From the perspective of data, live and spoofing features entangle with image content and are difficult to represent. From the perspective of models, adopting convolutional neural networks and deep learning models brings remarkable improvement of face anti-spoofing [43]. But these methods are biased to learn a texture-based representation rather than shape-based [11]. Because adversarial attacks will modify the image by adding noise, similar to change the texture, CNN-based models are vulnerable to adversarial examples. If these two perspectives are tackled well, such adversarial examples will be suitable to expose the adversarial vulnerability of face anti-spoofing models. Whether it is suitable for face anti-spoofing directly reflected in the improvement of attack success rate. So we propose Semantic Feature Augmentation (SFA) module to boost adversarial attacks in the context of face anti-spoofing.

How do we use adversarial examples to analyse adversarial vulnerability of face anti-spoofing models? For our community, we are concerned about classification accuracy and adversarial robustness of such accuracy at the same time. While so many annotations, geometric information and backbone networks can improve the accuracy to a similar level, figuring out which guarantees both accurate and robust is significant for data annotation strategy and model selection. However, most adversarial attacks [36,16,3] and benchmarks [8,31,9] towards specific tasks, draw conclusions by attacking the final results of models, only finding general and inexplicable problems of the target model. It is tricky for adversarial analysis if we fail to point out which part of the target face anti-spoofing model is vulnerable. So more fine-grained analysis method should be adopted to expose the explicit adversarial vulnerability of the model.

In order to achieve the above purposes and expose adversarial vulnerability of face anti-spoofing via semantic-aware and fine-grained adversarial attacks, **we made the following contributions in this paper:**

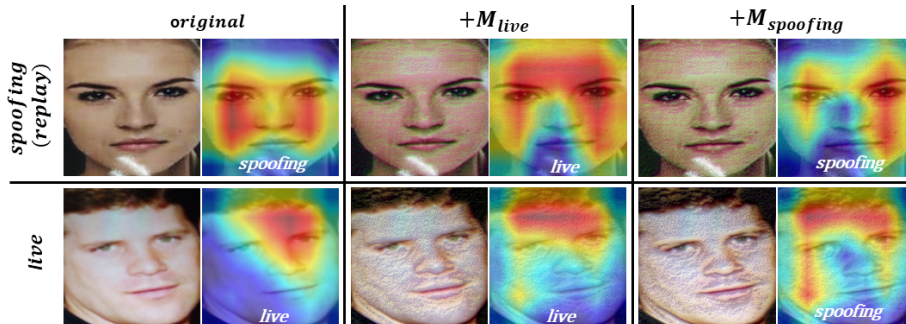


Fig. 1: Contrastive SFA maps of live and spoofing. A spoofing (replay) and live sample with their class activation maps (CAM) are shown in 1&2 columns, while 3&4 and 5&6 columns are the results added by M_{live} and $M_{spoofing}$ respectively. Spoofing activation region distribute around the face in the form of vertical lines. Live activate region distribute in the forehead area of face.

a. We propose Semantic Feature Augmentation (**SFA**) module to make adversarial noise semantic-aware to live and spoofing features, increasing the attack success rate by nearly 40% on average. As shown in Fig. 1, SFA not only can enhance the activation of target class, but also can enhance the activation of opposite class. In addition, SFA considers that neural networks are biased to texture features, so we use Local Binary Pattern (LBP) [6] to weight the noise. Previous work has rarely been able to boost adversarial attacks from both data and models at the same time, and this is why SFA can be so powerful and suitable to analyse face anti-spoofing models.

b. We use a fine-grained attack strategy to generate adversarial examples based on SFA and the multitask network with auxiliary information. Thus we can systematically expose the adversarial vulnerability of face anti-spoofing from three perspectives, which are annotations (facial attributes, spoofing types and illumination), geometric information (depth and reflection maps) and backbone networks. This can facilitate the selection of robust annotations and backbone networks. Such fine-grained adversarial examples translate the adversarial attack from a problem into a meaningful tool.

2 Background and related work

2.1 Face anti-spoofing

Face anti-spoofing is an important guarantee for the reliability of face recognition systems, especially in some security scenarios [43]. In early researches, face anti-spoofing algorithms were based on handcrafted features, such as LBP [41], HoG [33] and SURF [2]. Temporal features like eye-blinking [28] and lip motion [18] were also received attention. Methods based on different color spaces have also been proposed, such as HSV [2], YCbCr [2] and Fourier spectrum [20].

With the popularity of methods based on deep learning, CNNs have been used for feature extraction and classification, and these CNN-based methods achieved excellent performance [43], nearly 100% of accuracy in academic datasets. Auxiliary information including annotations [46] (facial attributes, spoofing types and illumination) and geometric maps [17] (depth and reflection map), were studied to assist the binary classification.

However, the emergence of adversarial attacks exposed the vulnerability of face anti-spoofing [38]. Different auxiliary information and backbone networks can indeed improve the binary classification accuracy of live and spoofing, but for such task related to security, its adversarial robustness should be paid attention to.

2.2 Adversarial attacks

Models based on deep learning are vulnerable to adversarial attacks, which is a popular research concern in recent years [1]. By adding the imperceptible noise to the original data, adversarial examples can mislead the classification easily [8]. Adversarial attacks can be divided into white-box and black-box attacks. White-box attacks [14] generated the adversarial perturbation by obtaining the gradient of model, while black-box attacks [24] focus on the transferability of adversarial examples.

In addition, some literature like [40,19] has explored the physical adversarial attacks in real-world scenes, making adversarial examples generated in digital domain can still mislead the target model after printing. However, considering that the aim of face anti-spoofing is to distinguish spoofing attacks in the physical domain and real-world diversity has been considered in the dataset, the adversarial robustness analysis of face anti-spoofing should focus on the digital domain first.

Besides being studied as a problem [32,29,42,25], adversarial examples can also be used as a tool to expose the vulnerability of the model, as well as measuring the impact of data distribution and network structure on the adversarial robustness [36,16,3,8,31,9].

2.3 Class activation map

Explicability of classification decision and localization made by the neural networks are obtained via the computation of class activation map (CAM) [34]. Furthermore, CAM and its following works [5,37,30,27,15] visualize class-relevant features in the form of heatmap, which is the reason why we select CAM [34] as a visualization tool to qualitatively demonstrate our experimental results.

3 Method

This section describes the details of our proposed methods. First, we take FGSM [14] as a representative method to introduce the generation process of adversarial examples in Sec. 3.1. Then, the training and inference pipeline of Semantic

Feature Augmentation (SFA) module is introduced in Sec. 3.2. Finally, we introduce the fine-grained adversarial attacks using SFA based on the multitask network with auxiliary information in Sec. 3.3.

3.1 Preliminary

The adversarial example x^{adv} is the image modified by the adversarial noise, and it can make the target model predict $f(x^{adv}) = v$ while such output is different from its label y . FGSM [14] is a one-step attack, which is formally defined by

$$x^{adv} = x + \epsilon \cdot \text{sign}(\nabla_x L(v, y)) \tag{1}$$

where x , ϵ and $L(\cdot)$ denote the input image, max perturbation scale and loss function. Because FGSM generates adversarial examples efficiently, we use FGSM as the basic adversarial attack in Sec. 3.3.

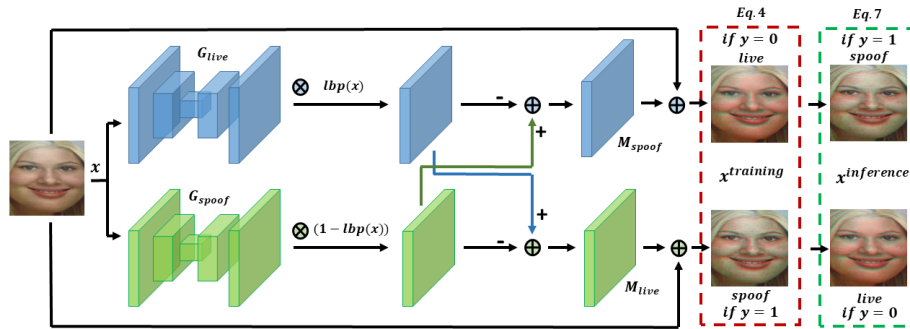


Fig. 2: The pipeline of Semantic Feature Augmentation (SFA) module. G_{live} and $G_{spoofing}$ are used to generate live and spoofing activation maps, and LBP is used for texture filtering. The last part is different at training stage (See Eq. 4) and inference stage (See Eq. 7).

3.2 Semantic Feature Augmentation (SFA)

Face anti-spoofing is tricky because live and spoofing features are difficult to be extracted. [44] separates latent representation into live clues and content, while [21] tries to disentangle the spoofing traces from input faces. However, their methods have two respects of drawbacks: (a) Reconstruction and synthesis brings massive burden of optimization. (b) They rarely consider that CNN-based models are biased to texture features [11].

So Semantic Feature Augmentation (SFA) module is proposed to address the problems above. SFA not only changes the activation of target class, but also considers the activation of opposite class. In addition, SFA considers that neural

networks are biased to texture feature [11], so we use Local Binary Pattern (LBP) [6] to weight the activation maps. Previous work has rarely been able to boost adversarial attacks from both data and models, and this is why SFA can be so powerful and suitable to face anti-spoofing models.

Next, we will introduce each part of the pipeline shown in Fig. 2:

Generator Two variational autoencoders, denoted as G_{live} and $G_{spoofing}$, are used for generating live and spoofing activation maps (M_{live} and $M_{spoofing}$) respectively. Then, the activation maps output by G_{live} and $G_{spoofing}$ will be weighted by LBP [6] denoted as $lbp(\cdot)$. To be specific, for the input image x , the activation maps M_{live} and $M_{spoofing}$ can be obtained by the following formula:

$$M_{live}(x) = lbp(x) \cdot G_{live}(x) - [1 - lbp(x)] \cdot G_{spoofing}(x) \quad (2)$$

$$M_{spoofing}(x) = -lbp(x) \cdot G_{live}(x) + [1 - lbp(x)] \cdot G_{spoofing}(x) \quad (3)$$

Discriminator The pre-trained face anti-spoofing model will be chosen to be the discriminator, denoted as D . The parameters of this target model are fixed in the process of optimizing the generator.

Training and loss function The modified image $x_i^{training}$ for optimizing G_{live} and $G_{spoofing}$, can be generated by Eq. 4, which input image x_i is added by activation map opposite to its label:

$$x_i^{training} = x_i + y_i \cdot M_{live}(x_i) + (1 - y_i) \cdot M_{spoofing}(x_i) \quad (4)$$

where $[x_i, y_i]_{i=1}^N$ is a batch of training data with labels. Note that $y_i=0$ if the input image is live, otherwise $y_i=1$.

The training objective is to make the $x_i^{training}$, inferred by the discriminator D , consistent with the opposite label. As shown below, the Binary Cross Entropy is adopted:

$$L_1 = -\frac{1}{N} \sum_{i=1}^N [(1 - y_i) \cdot \log(D(x_i^{training})) + y_i \cdot \log(1 - D(x_i^{training}))] \quad (5)$$

To better introduce our method and experimental results in the following sections, we denote Semantic Feature Augmentation module as $SFA(\cdot)$, which can generate the activation map same as its label:

$$SFA(x) = y \cdot M_{spoofing}(x) + (1 - y) \cdot M_{live}(x) \quad (6)$$

$$x^{inference} = x + SFA(x) \quad (7)$$

3.3 Fine-grained adversarial attacks based on SFA

In order to fully mine the impact of data annotation and auxiliary information on the adversarial robustness of face anti-spoofing, we adopt the multitask network with auxiliary information [46] as basic model.

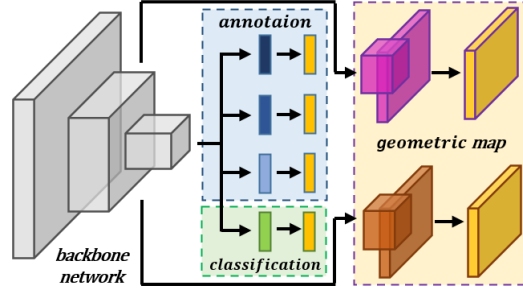


Fig. 3: Multitask network with auxiliary information.

As shown in Fig. 3, the backbone network is marked gray, and the last logits are output to four fully-connected layers, to obtain the vector v_f , v_t , v_i and v_c , which represents facial attributes, spoofing types, illumination and binary classification of live and spoofing. Their corresponding ground truth is marked yellow. The three annotation vectors are compared with label y_f , y_t and y_i , thus we get the semantic loss function L_a as follows:

$$L_a = \lambda_f \cdot L_f(v_f, y_f) + \lambda_t \cdot L_t(v_t, y_t) + \lambda_i \cdot L_i(v_i, y_i) \quad (8)$$

where L_t and L_i use Softmax Cross Entropy, and L_f uses Binary Cross Entropy. Set $\lambda_f = 1$, $\lambda_t = 0.1$, $\lambda_i = 0.01$.

Furthermore, reflection map v_r and depth map v_d are captured by two geometric map generators, which consist of a Conv 3×3 followed by an upsample to 14×14 . According to [46], for the depth map of the sample labeled live, its ground truth y_d is obtained by PRNet [10], while the depth map of sample labeled spoofing is zero. The method proposed in [45] is adopted to generate the ground truth of reflection map of the sample labeled spoofing, and the reflection map of sample labeled live is zero. Therefore, we can get the following geometric loss function L_g :

$$L_g = \lambda_d \cdot L_d(v_d, y_d) + \lambda_r \cdot L_r(v_r, y_r) \quad (9)$$

where, L_d and L_r are Mean Square Error. λ_d and λ_r are set to 0.1. Use Softmax Cross Entropy as L_c , thus we can get the final optimization objective:

$$L_2 = L_c(v_c, y_c) + L_a + L_g \quad (10)$$

Based on the structure mentioned in Fig. 3, the annotation vectors, classification vector and geometric maps can be obtained. From the perspective of auxiliary information (annotation vectors and geometric maps), we attack different parts of the last layer, and analyse the adversarial robustness of the target model. The adversarial vulnerability of different auxiliary information can be illustrated from the change of classification accuracy. FGSM[14] is adopted as the basic method to generate these fine-grained adversarial examples:

$$x_s^{adv} = x + \epsilon \cdot \text{sign}(\nabla_{x+SF A(x)} L_s(v_s, y_s)) \quad (11)$$

where $s \in \{f, t, i, d, r, c\}$ respectively represent the facial attributes, spoofing types, illumination, depth map, reflection map and classification. ϵ indicates the step of the attack. Adversarial perturbation is generated based on the images modified by SFA.

Furthermore, replacing the backbone network with different state-of-art models, can provide us with a new perspective to study adversarial vulnerability of face anti-spoofing models, from the effects of backbone structures.

4 Experiment

4.1 Experimental setting

The purpose of our paper is to expose adversarial vulnerability of face anti-spoofing from the fine-grained perspective and figure out which part of the target models is vulnerable. So our experiments use CelebA-spoof [46] as the dataset, which has three significant advantages: (a) Large-scale: CelebA-spoof comprises of 625,537 pictures of 10,177 subjects. (b) Diversity: The spoofing images are captured from 8 scenes (2 environments \times 4 illumination conditions) with more than 10 sensors. (c) Annotation richness: CelebA-spoof contains 10 spoofing type annotations, as well as the 40 attribute annotations inherited from the original CelebA [23] dataset. These three advantages are helpful for us to construct the required experimental scenarios, and the experimental results based on this large-scale dataset are more general.

In order to improve the experimental efficiency, the visualization results presented in this paper are generated by FGSM [14], because the FGSM is an one-step attack and its generation is efficient.

The attack success rate and classification accuracy are metrics for the performance of adversarial attacks, while mean square error is taken to measure the change of each feature output. The results predicted by the target model is correct when the output after Softmax is the same as the ground truth.

Table 1: The attack success rates of different adversarial attacks without and with SFA.

adversarial attacks	attack success rate	
	without SFA	with SFA
<i>FGSM</i> ($\epsilon = 0.06$) [14]	0.6578	0.9046 \uparrow
<i>C&W</i> ($\epsilon = 0.06$) [4]	0.6925	0.8812 \uparrow
<i>Spatial</i> ($\epsilon = 0.06$) [39]	0.4786	0.9443 \uparrow
<i>PGD</i> _{l2} ($\epsilon = 0.1$) [26]	0.4575	0.7325 \uparrow
<i>Sparse</i> ($\epsilon = 0.2$) [7]	0.0000	0.6088 \uparrow

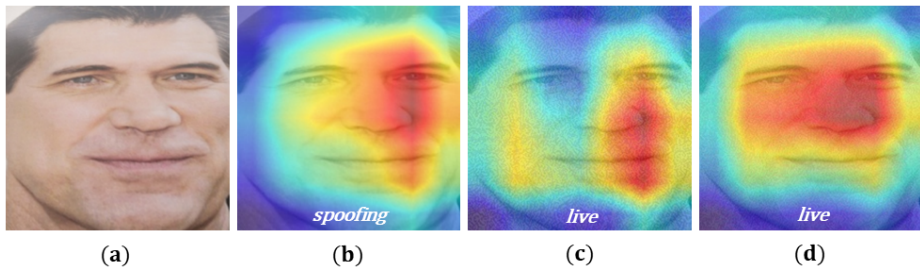


Fig. 4: Differences of adversarial attacks without and with SFA. (a) Original spoofing image. (b) CAM of the original image. (c) CAM of the adversarial image without SFA (almost the same as Fig. 4(b)). (d) CAM of the adversarial image with SFA (completely different from Fig. 4(b)). SFA makes the adversarial perturbation more concentrate on the semantic features and boosts adversarial attacks, so attacks with SFA do change class-related information of input images. Such effects and differences are illuminated by CAM, which can explicitly locate the classification decision.

4.2 Effectiveness analysis of SFA

Semantic Feature Augmentation (SFA) module is designed for the specific and difficult binary classification task faced by face anti-spoofing. Its characteristic is to learn the activation maps of the target model towards classes of live and spoofing, by constructing positive and negative samples weighted by the texture filter. With the help of SFA, adversarial perturbation can be added more semantic-aware to live and spoofing features. In this way, it can not only improve the attack success rate, but also make fine-grained adversarial attacks more related to live and spoofing decision boundary.

In this section, we first show that SFA can generate two different maps for one image (See Fig. 1), and study the effect of SFA on different adversarial attacks, to verify that SFA can improve the attack success rate (See Tab. 1 and Fig. 4). Then, we compare SFA with different methods of class activation map (CAM) and data augmentation (See Tab. 2), to illustrate the advantages of SFA over previous methods. Finally, ablation experiments on the texture filter are carried out to show the necessity of it (See Tab. 3).

Contrastive activation maps of live and spoofing SFA can generate two different maps for one image, corresponding to live and spoofing respectively, as shown in Fig. 1. According to numerous empirical observations on the visualization of experimental results, spoofing activation tends to distribute at the edge and has the law of quadrilateral grid. For the live activation, the inner region of the face is stronger, especially the forehead. To boost the adversarial attacks, the $SFA(\cdot)$ denoted in Eq. 6 adds activation map with the same label to the input image.

Different adversarial attacks with SFA As shown in Tab. 1, the success attack rates of different adversarial attacks [14,26,7,4,39] have improved a lot with the help of SFA. As shown in Fig. 4, we then visualize a spoofing example with its adversarial examples generated without and with SFA.

Differences between SFA, data augmentation and class activation map

As shown in Tab. 2, we select typical methods of data augmentation and class activation map (CAM) [34,5,37,30,27,15] to compare with SFA, and take FGSM [14] as the adversarial attack. Geometric transformations made by data augmentations diversify the gradients, but have little effect on the enhancement of semantic-aware features. Both CAM and SFA have studied the activation of the model towards specific classes, but CAM only consider the unique class. When SFA generates activation maps, it not only enhances the target class, but also considers the opposite class.

Table 2: The attack success rates of FGSM [14] with SFA, data augmentation and class activation map.

FGSM [14] + data augmentation		FGSM [14] + class activation map	
method	attack success rate	method	attack success rate
none	0.6578	none	0.6578
vertical flip	0.7313	Gradcam[34]	0.7375
horizontal flip	0.7063	Gradcam++[5]	0.7625
rotation(30°)	0.7563	Scorecam[37]	0.2875
brightness	0.6938	Ablationcam[30]	0.7375
hue	0.7250	Eigencam[27]	0.8000
contrast	0.6875	Layercam[15]	0.7625
SFA	0.9046	SFA	0.9046

Ablation of texture filter Texture filter is necessary for SFA. CNNs are biased to texture features [11], which is the vulnerability of methods based on deep learning. Considering changing texture features can improve the success rate of adversarial attacks, as shown in Tab. 3.

Table 3: The attack success rates of SFA without and with LBP.

method	attack success rate
FGSM [14]+SFA(without LBP)	0.7050
FGSM [14]+SFA(with LBP)	0.9046

4.3 How to use fine-grained adversarial examples to analyse adversarial vulnerability of face anti-spoofing models?

Analysis of auxiliary information Take the Resnet-18 [12] trained on CelebA-spoof [46] as the target model, and FGSM [14] is used as the method of adversarial attacks. As shown in Tab. 4, SFA can improve the success attack rate of all parts except facial attributes.

Table 4: The accuracy of Resnet-18 when different annotation vectors and geometric maps are attacked.

attacked parts	accuracy	
	without SFA	with SFA
facial attributes	0.3659	0.5799 ↑
spoofing types	0.3545	0.2441 ↓
illumination	0.3525	0.2321 ↓
depth map	1.0	0.3306 ↓
reflection map	0.9999	0.3343 ↓
classification	0.3422	0.0954 ↓

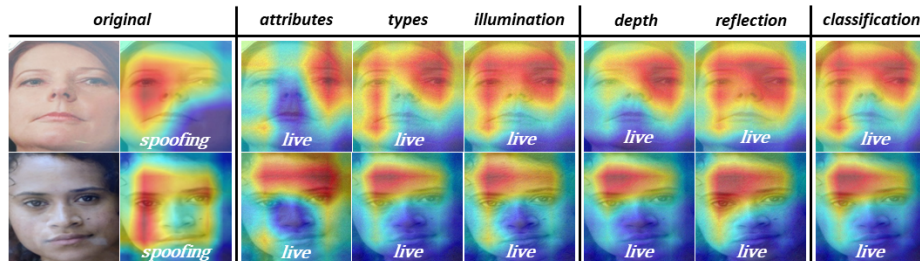


Fig. 5: Visualization of adversarial attacks on different annotation vectors and geometric maps of spoofing data.

As shown in Fig. 5, for facial attributes, although the adversarial attack has perturb the feature vector of facial attributes, it does not change the pattern of spoofing activation, different from other annotation vectors and geometric maps. This shows that spoofing types, illumination, depth map and reflection map are more relevant to the ground truth decision boundary. The interpretation of such differences can be shown in Fig. 6.

Analysis of backbone networks According to the latest survey [43], we select VGG-13 [35], Resnet-18 [12], Densenet-121 [13] and Swin Transformer [22] as four representative backbone networks. The checkpoints of the target models

Table 5: The accuracy of different backbone networks when their annotation vectors and geometric maps are attacked.

backbone networks		VGG [35]	Resnet [12]	Densenet[13]	Swin Transformer[22]
original accuracy		0.9416	0.9988	0.9971	0.9989
annotation	facial attributes	0.7849	0.5799	0.6598	0.4623
	spoofing types	0.3462	0.2441	0.3838	0.1684
	illumination	0.2736	0.2321	0.2999	0.2965
geometric	depth map	0.4483	0.3306	0.3686	0.3302
	reflection map	0.6484	0.3343	0.3304	0.3408
classification		0.2876	0.0954	0.2744	0.0962

are trained on CelebA-spoof [46], and the accuracy of each model is close to 100%.

Analysis of different backbone networks in the task of face anti-spoofing will be carried out in two dimensions: (a) The changes of accuracy when different annotation and geometric parts are attacked. (b) The changes of each annotation and geometric part when the binary classification of live and spoofing is attacked.

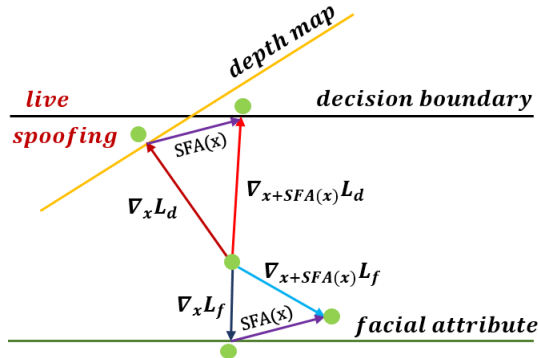


Fig. 6: The interpretation of differences between facial attribute boundary and depth map boundary. Considering a spoofing sample, depth map boundary has a higher correlation with the decision boundary, so SFA can make it pass through such decision boundary. However, facial attribute boundary has low correlation with the decision boundary of live and spoofing. Even if SFA biases the example towards that decision boundary, it fails crossing such boundary.

a. Adversarial attacks on different annotation and geometric parts

Attack the different annotations (facial attributes, spoofing types and illumination), geometric maps (depth and reflection) and binary classification in turn. The changes of accuracy of each backbone networks are shown in Tab. 5.

Through the comparison of columns, the correlation of each feature vector towards the binary classification of live and spoofing can be reflected. The accu-

racy of facial attributes deserves attention, while attacking facial attributes has less impact on the results of binary classification. Such phenomenon exists in all four backbone networks. This shows that the annotation of facial attributes is redundant annotation for the binary classification of live and spoofing.

Then, analyse other attacked parts of different backbone networks from the rows. Interestingly, VGG and Densenet have better adversarial robustness when the accuracy is approximately equal.

Therefore, when selecting backbone networks for specific tasks, we should handle the trade-off between accuracy and adversarial robustness.

Table 6: The changes of annotation vectors and geometric maps when the binary classification of the target model is attacked.

backbone networks		VGG [35]	Resnet [12]	Densenet[13]	Swin Transformer[22]
annotation	facial attributes	0.39	0.20	0.07	0.20
	spoofing types	0.70	2.40	0.03	0.20
	illumination	12.80	6.60	0.70	8.40
geometric	depth map	4.21	0.10	0.04	0.00
	reflection map	2.30	13.60	1.80	0.40

b. Adversarial attacks on the binary classification

Tab. 6 shows the changes of each annotation vector and geometric map of different backbone networks when the binary classification of live and spoofing is attacked. The Mean Square Error is used as a metric of change. To have better comparability among various feature vectors, the error is divided by l_2 -norm of output vectors and maps.

Observing the rows, the structure of VGG can enhance the correlations between different feature parts, resulting obvious changes of other features when the binary classification is attacked.

Through the comparison of columns, the parts related to light tend to change a lot, including illumination and reflection maps. According to [17] and human perception, the differences of light between live and spoofing samples are obvious, especially in spoofing type such as replay. Furthermore, for RGB images, although the depth information is used in our experiments, the change of depth map is small. It is worth noting that in the application scenario where the most existing commercial cameras collect RGB images, the way of making the networks learn to use depth information is an important problem when tackling binary classification of live and spoofing.

5 Conclusion and ethical concern

Conclusion In this paper, we propose Semantic Feature Augmentation (SFA) module, which can increase the attack success rate by nearly 40% on average. Then, we generate fine-grained adversarial based on SFA in the context of face

anti-spoofing. We use such tools to evaluate three annotations, two geometric maps and four backbone networks, drawing several meaningful and practical results. These novel perspectives can help our community to select annotations, geometric information and backbone networks with better adversarial robustness when solving the task of face anti-spoofing, so as to improve the reliability of biometric authentication systems. In the future, we will explore the adversarial learning based our adversarial attack formulation.

Ethical concern Before launching defense, studying attacks is significantly necessary. This paper guides the adversarial examples as a tool to analyse face anti-spoofing models. We aim to improve the positive impact of the adversarial examples. The methods proposed in our paper can deepen our understanding of data and models, instead of undermining the security of current face recognition systems.

References

1. Akhtar, N., Mian, A.: Threat of adversarial attacks on deep learning in computer vision: A survey. *Ieee Access* **6**, 14410–14430 (2018)
2. Boulkenafet, Z., Komulainen, J., Hadid, A.: Face antispoofing using speeded-up robust features and fisher vector encoding. *IEEE Signal Processing Letters* **24**(2), 141–145 (2016)
3. Carlini, N., Athalye, A., Papernot, N., Brendel, W., Rauber, J., Tsipras, D., Goodfellow, I., Madry, A., Kurakin, A.: On evaluating adversarial robustness. *arXiv preprint arXiv:1902.06705* (2019)
4. Carlini, N., Wagner, D.: Towards evaluating the robustness of neural networks. In: 2017 *IEEE Symposium on Security and Privacy (SP)*. pp. 39–57. *IEEE* (2017)
5. Chattopadhyay, A., Sarkar, A., Howlader, P., Balasubramanian, V.N.: Grad-cam++: Generalized gradient-based visual explanations for deep convolutional networks. In: 2018 *IEEE Winter Conference on Applications of Computer Vision (WACV)*. pp. 839–847. *IEEE* (2018)
6. Chingovska, I., Anjos, A., Marcel, S.: On the effectiveness of local binary patterns in face anti-spoofing. In: 2012 *BIOSIG-proceedings of the international conference of biometrics special interest group (BIOSIG)*. pp. 1–7. *IEEE* (2012)
7. Croce, F., Hein, M.: Sparse and imperceivable adversarial attacks. In: *Proceedings of the IEEE/CVF International Conference on Computer Vision*. pp. 4724–4732 (2019)
8. Dong, Y., Fu, Q.A., Yang, X., Pang, T., Su, H., Xiao, Z., Zhu, J.: Benchmarking adversarial robustness on image classification. In: *CVPR*. pp. 321–331 (2020)
9. Eger, S., Benz, Y.: From hero to z\`eroe: A benchmark of low-level adversarial attacks. *arXiv preprint arXiv:2010.05648* (2020)
10. Feng, Y., Wu, F., Shao, X., Wang, Y., Zhou, X.: Joint 3d face reconstruction and dense alignment with position map regression network. In: *Proceedings of the European Conference on Computer Vision (ECCV)*. pp. 534–551 (2018)
11. Geirhos, R., Rubisch, P., Michaelis, C., Bethge, M., Wichmann, F.A., Brendel, W.: Imagenet-trained cnns are biased towards texture; increasing shape bias improves accuracy and robustness. *arXiv preprint arXiv:1811.12231* (2018)

12. He, K., Zhang, X., Ren, S., Sun, J.: Deep residual learning for image recognition. In: Proceedings of the IEEE conference on computer vision and pattern recognition. pp. 770–778 (2016)
13. Huang, G., Liu, Z., Van Der Maaten, L., Weinberger, K.Q.: Densely connected convolutional networks. In: Proceedings of the IEEE conference on computer vision and pattern recognition. pp. 4700–4708 (2017)
14. Huang, S., Papernot, N., Goodfellow, I., Duan, Y., Abbeel, P.: Adversarial attacks on neural network policies. arXiv preprint arXiv:1702.02284 (2017)
15. Jiang, P.T., Zhang, C.B., Hou, Q., Cheng, M.M., Wei, Y.: Layercam: Exploring hierarchical class activation maps for localization. *IEEE Trans. Image Process.* **30**, 5875–5888 (2021)
16. Jiang, Y., Bansal, M.: Avoiding reasoning shortcuts: Adversarial evaluation, training, and model development for multi-hop qa. arXiv preprint arXiv:1906.07132 (2019)
17. Kim, T., Kim, Y., Kim, I., Kim, D.: Basn: Enriching feature representation using bipartite auxiliary supervisions for face anti-spoofing. In: Proceedings of the IEEE/CVF International Conference on Computer Vision Workshops. pp. 0–0 (2019)
18. Kollreider, K., Fronthaler, H., Faraj, M.I., Bigun, J.: Real-time face detection and motion analysis with application in “liveness” assessment. *IEEE Transactions on Information Forensics and Security* **2**(3), 548–558 (2007)
19. Komkov, S., Petiushko, A.: Advhat: Real-world adversarial attack on arcface face id system. In: 2020 25th International Conference on Pattern Recognition (ICPR). pp. 819–826. IEEE (2021)
20. Li, J., Wang, Y., Tan, T., Jain, A.K.: Live face detection based on the analysis of fourier spectra. In: Biometric technology for human identification. vol. 5404, pp. 296–303. International Society for Optics and Photonics (2004)
21. Liu, Y., Stehouwer, J., Liu, X.: On disentangling spoof trace for generic face anti-spoofing. In: European Conference on Computer Vision. pp. 406–422. Springer (2020)
22. Liu, Z., Lin, Y., Cao, Y., Hu, H., Wei, Y., Zhang, Z., Lin, S., Guo, B.: Swin transformer: Hierarchical vision transformer using shifted windows. arXiv preprint arXiv:2103.14030 (2021)
23. Liu, Z., Luo, P., Wang, X., Tang, X.: Large-scale celebfaces attributes (celeba) dataset. Retrieved August **15**(2018), 11 (2018)
24. Ma, C., Chen, L., Yong, J.H.: Simulating unknown target models for query-efficient black-box attacks. In: Proceedings of the IEEE/CVF Conference on Computer Vision and Pattern Recognition. pp. 11835–11844 (2021)
25. Ma, T., Li, D., Wang, W., Dong, J.: Face anonymization by manipulating decoupled identity representation. arXiv preprint arXiv:2105.11137 (2021)
26. Madry, A., Makelov, A., Schmidt, L., Tsipras, D., Vladu, A.: Towards deep learning models resistant to adversarial attacks. arXiv preprint arXiv:1706.06083 (2017)
27. Muhammad, M.B., Yeasin, M.: Eigen-cam: Class activation map using principal components. In: 2020 International Joint Conference on Neural Networks (IJCNN). pp. 1–7. IEEE (2020)
28. Pan, G., Sun, L., Wu, Z., Lao, S.: Eyeblink-based anti-spoofing in face recognition from a generic webcam. In: 2007 IEEE 11th international conference on computer vision. pp. 1–8. IEEE (2007)
29. Pang, T., Yang, X., Dong, Y., Su, H., Zhu, J.: Bag of tricks for adversarial training. arXiv preprint arXiv:2010.00467 (2020)

30. Ramaswamy, H.G., et al.: Ablation-cam: Visual explanations for deep convolutional network via gradient-free localization. In: Proceedings of the IEEE/CVF Winter Conference on Applications of Computer Vision. pp. 983–991 (2020)
31. Rauber, J., Zimmermann, R., Bethge, M., Brendel, W.: Foolbox native: Fast adversarial attacks to benchmark the robustness of machine learning models in pytorch, tensorflow, and jax. *Journal of Open Source Software* **5**(53), 2607 (2020)
32. Rice, L., Wong, E., Kolter, Z.: Overfitting in adversarially robust deep learning. In: International Conference on Machine Learning. pp. 8093–8104. PMLR (2020)
33. Schwartz, W.R., Rocha, A., Pedrini, H.: Face spoofing detection through partial least squares and low-level descriptors. In: 2011 International Joint Conference on Biometrics (IJCB). pp. 1–8. IEEE (2011)
34. Selvaraju, R.R., Cogswell, M., Das, A., Vedantam, R., Parikh, D., Batra, D.: Grad-cam: Visual explanations from deep networks via gradient-based localization. In: Proceedings of the IEEE international conference on computer vision. pp. 618–626 (2017)
35. Simonyan, K., Zisserman, A.: Very deep convolutional networks for large-scale image recognition. *arXiv preprint arXiv:1409.1556* (2014)
36. Tong, L., Chen, Z., Ni, J., Cheng, W., Song, D., Chen, H., Vorobeychik, Y.: Facesec: A fine-grained robustness evaluation framework for face recognition systems. In: Proceedings of the IEEE/CVF Conference on Computer Vision and Pattern Recognition. pp. 13254–13263 (2021)
37. Wang, H., Wang, Z., Du, M., Yang, F., Zhang, Z., Ding, S., Mardziel, P., Hu, X.: Score-cam: Score-weighted visual explanations for convolutional neural networks. In: Proceedings of the IEEE/CVF conference on computer vision and pattern recognition workshops. pp. 24–25 (2020)
38. Wu, H., Liu, A.T., Lee, H.y.: Defense for black-box attacks on anti-spoofing models by self-supervised learning. *arXiv preprint arXiv:2006.03214* (2020)
39. Xiao, C., Zhu, J.Y., Li, B., He, W., Liu, M., Song, D.: Spatially transformed adversarial examples. *arXiv preprint arXiv:1801.02612* (2018)
40. Xiao, Z., Gao, X., Fu, C., Dong, Y., Gao, W., Zhang, X., Zhou, J., Zhu, J.: Improving transferability of adversarial patches on face recognition with generative models. In: Proceedings of the IEEE/CVF Conference on Computer Vision and Pattern Recognition. pp. 11845–11854 (2021)
41. Yang, J., Lei, Z., Liao, S., Li, S.Z.: Face liveness detection with component dependent descriptor. In: 2013 International Conference on Biometrics (ICB). pp. 1–6. IEEE (2013)
42. Yang, S., Wang, W., Cheng, Y., Dong, J.: A systematical solution for face de-identification. In: Chinese Conference on Biometric Recognition. pp. 20–30. Springer (2021)
43. Yu, Z., Qin, Y., Li, X., Zhao, C., Lei, Z., Zhao, G.: Deep learning for face anti-spoofing: a survey. *arXiv preprint arXiv:2106.14948* (2021)
44. Zhang, K.Y., Yao, T., Zhang, J., Tai, Y., Ding, S., Li, J., Huang, F., Song, H., Ma, L.: Face anti-spoofing via disentangled representation learning. In: European Conference on Computer Vision. pp. 641–657. Springer (2020)
45. Zhang, X., Ng, R., Chen, Q.: Single image reflection separation with perceptual losses. In: Proceedings of the IEEE conference on computer vision and pattern recognition. pp. 4786–4794 (2018)
46. Zhang, Y., Yin, Z., Li, Y., Yin, G., Yan, J., Shao, J., Liu, Z.: Celeba-spoof: Large-scale face anti-spoofing dataset with rich annotations. In: ECCV. pp. 70–85. Springer (2020)